Surface Segregation in Polymer Blends: A Monte Carlo Simulation

P. Cifra,† F. E. Karasz,* and W. J. MacKnight‡

Polymer Institute, Slovak Academy of Sciences, Dúbravská cesta 842 36, Bratislava, Czechoslovakia, and Department of Polymer Science and Engineering, University of Massachusetts, Amherst, Massachusetts 01003

Received February 6, 1992

ABSTRACT: A Monte Carlo (MC) simulation of surface enrichment in polymer blends is presented. The algorithm introduced by Madden is used in this simulation, in which a compressible blend is condensed against a solid wall, with the surface of the blend forming an interface with holes (or solvent) that is parallel to the wall. Three regimes in the mixture are thus recognized: the interface at the wall, the bulk regime, and the interface with the vacuum (or solvent) at the surface of the mixture. Under certain conditions, enrichment of one of the components is observed, both at the surface and close to the wall. We find that the surface enrichment even in systems with the same cohesive energy in both components is driven by intermacromolecular interaction and asymmetric composition effects. A smaller part of the driving force arises from the difference in coil sizes between components, with the surface layer of the blend containing an excess of the component with the smaller coil size. A difference in coil sizes in a mixture containing polymers of equal chain length occurs in systems of asymmetric composition and with favorable interaction between components: in this case the majority chains act as a favorable solvent for the minority chains. In such asymmetric compositions, the minority chains move from the surface layers into the more favorable bulk regime. The results are compared with recent mean-field (MF) theory predictions and with those of available experiments. An important finding is that this type of segregation in miscible blends can occur well within the one-phase region of the phase diagram as well as at its more expected location close to the binodal region.

I. Introduction

Interface and surface properties are known to play an important role in solid polymers, polymer blends, and composites. Despite their importance, not much is known about interfaces on the microscopic level. In this contribution we investigate surface segregation (enrichment) in polymer blends—segregation that can have a large effect on the surface properties of mixtures. It has been known[1,2] for some time that enrichment near a polymer surface by one of the components of a mixture can occur if the blend lies close to the coexistence curve of the corresponding phase diagram. If the enriched surface layer is thick, then the surface properties of the mixture are indeed largely those of that component. High-molecular-weight systems can be expected to produce a thicker enrichment layer than that of low-molecular-weight liquids and also to show some correlation between the thickness of the layer and the size of polymer coils. Initial activity in this field has been theoretical.[1,2] Lagging experimental data reflect the difficulty of studying the interface, especially the surface composition profile, in a mixture. Recent experiments using neutron reflection[3-5] and deuterated polymers have measured concentration profiles and surface demixing for blends with small positive Flory interaction parameters. These results have been interpreted according to mean-field (MF) theory. More recently Kumar et al.[6] have reported results based on a mean-field lattice treatment for surface enrichment in athermal polymer mixtures at the wall–polymer interface where this effect results from the difference in chain lengths of components. From their analysis, it follows that the effect attributable to entropic considerations is small, leading to excess surface concentrations of only ~1%. On the other hand, inclusion of segmental interactions affects the surface to a major extent.[7]

As mentioned above, knowledge of the surface behavior of a miscible polymer blend is limited and can be characterized as follows: if there exists a difference in surface free energies of the blend components, this difference may lead to surface demixing in a mixture that is otherwise miscible in the bulk regime. This surface segregation extends beyond the surface layer to a depth that depends on the bulk miscibility of the blend. If the temperature and composition of the blend lies close to the binodal region on the phase diagram (i.e., close to bulk phase demixing), the demixed layer extends more deeply into the bulk material. This behavior is expected: the surface free energy difference initiates a demixing at the surface, and this effect penetrates into the material to an extent dependent on the tendency of this single bulk phase to demix. The present results acquired by Monte Carlo simulation calculations imply a somewhat different behavior. For example, surface segregation is found in systems in which there is no difference in the surface interactions of the two components. Moreover, this effect is enhanced by a more favorable interaction between the components (e.g., for a strongly negative χ, deep in the one-phase region of the phase diagram). We outline possible explanations in section III.

In the computation we employed the unique algorithm developed by Madden,[8] which allowed us to study the interfaces in a compressible mixture in a grand canonical ensemble (opened to exchange of voids only); this method is described in section II. The number of complicating factors that affect segregation was decreased by simulating a system with no differences between surface or cohesive energies of the components. Surprisingly, we found surface enrichment even here, under certain conditions. The results are discussed in section III in terms of differences in coil dimensions, cooperative effects of interactions and composition, and the deformation and orientation of coils at the interface.

* To whom correspondence should be addressed at the University of Massachusetts.
† Slovak Academy of Sciences.
‡ University of Massachusetts.

0024-9297/92/2225-4895$03.00/0

II. Simulation Method

The conventional simulation of bulk condensed media, which uses isotropic periodic boundary conditions, is unsuitable for the simulation of interfaces. In fact, one problem with this method is the effective simulation of an inhomogeneous two-phase system. The use of a grand canonical ensemble overcomes this restriction. The semigrand canonical algorithm of Sariban and Binder[9,10] allows for the transformation of one species in the mixture into another. Applied to a symmetric mixture containing polymers of the same chain length, the algorithm simulates one-half of the symmetric phase diagram for a two-phase mixture in equilibrium, that is, it simulates only a one-phase regime. Another constraint of this algorithm is that it permits exchange only between chains and not between chains and solvent (holes); hence, these systems are incompressible. The interface between two coexisting polymer melts was recently investigated by Olaj et al.,[11] who used antiperiodic boundary conditions perpendicular to the interface. However, the incompressibility condition was still maintained. To elaborate our previous MC studies[12] of polymer blends, we therefore turned to the slab geometry introduced by Madden,[8] which is suitable for the study of coexisting phases—and thus also the interface between such phases—and can be used to simulate compressible systems.

In our simulation we used a rectangular section of a cubic lattice with dimensions $(x, y, z) = (22, 22, 50)$. At the first layer in the z direction, $z = 1$, we imposed a hard wall by completely filling all the sites on this plane. Periodic boundary conditions were used only in the x and y directions. The wall presented an attractive interaction toward both components A and B used in the blend simulation. The purpose of this adsorbing wall was to fix the condensed polymer phase in space and also to create a regular planar interface. All interactions were assumed to be short-range, i.e., nearest-neighbor interactions that take place between the segments on the lattice and that depend on the identity of the segments occupying the neighboring sites. Dimensionless interaction energies, reduced by kT, were used: the wall–polymer segment was given an interaction energy e_w; the respective cohesive energies in the mixture were designated e_{AA} and e_{BB}; interaction between unlike polymer segments was denoted by the variable e_{AB}. We arbitrarily defined A as the minority and B as the majority component. Interaction of either type of polymer segment with the vacuum (holes, solvent) was athermal. The net interaction between polymers was expressed through the segmental interaction parameter $\chi_{AB} = (Z - 2)\Delta e_{AB}$, where $\Delta e_{AB} = e_{AB} - (e_{AA} + e_{BB})/2$ and Z denoted the lattice coordination number; in the present calculations, $e_{AA} = e_{BB}$ and only e_{AB} was varied. All interactions were superimposed on a basic excluded volume intra- and interchain interaction based on site occupancy. The wall adsorption energy was set equal to the cohesive energy of the pure bulk components, i.e., $e_w = e_{AA} = e_{BB}$, so that a polymer segment located near the wall had an energy approximately equal to that of one in the bulk systems.

The simulation process itself consisted of two steps: (1) The first step was the buildup of a suitable multichain initial configuration. For this we used a second, temporary, wall, located at $z = 36$. This wall was noninteractive, and in this step all other interactions were set equal to zero. The second wall was used to confine the system in the absence of interactions and adsorption, in order to mix the system athermally and to form an initial arbitrary interface with the vacuum. In this study, 484 chains, each consisting of $N = 30$ segments, and initially extended parallel to the z axis, were allowed to mix within the volume between the walls by using reptation moves. (2) In step 2, all the calculations of simulated states discussed below started from the random multichain configuration obtained in step 1. For these calculations, the second wall was moved to $z = 50$ and, because chains never penetrated to this extent along this axis, became inconsequential to all further calculations. In a typical simulation the blend composition x_A (i.e., fraction of A chains relative to the total number of chains) was set to a constant value, randomly assigning an A or a B to each chain from the total array until the desired composition was achieved. Next, the interaction energies were introduced. The system was then equilibrated through the normal chain conformational moves, each state being defined by the given energy parameters. As a consequence of the favorable cohesive energies, when equilibrium was reached, there was a well-defined bulk concentration (expressed, for example, in terms of an occupied volume fraction) in the interior of the slab in equilibrium with the reservoir of holes above the blend. This system thus represented a semigrand canonical ensemble with respect to voids, because it was open to the exchange of voids between the bulk and the vacuum above the condensed phase. As already noted, in this simulation we were particularly interested in the composition of the interface at the surface of the polymer mixture.

Although the geometric portion of the simulation algorithm incorporated Madden's algorithm, we preferred to use alternative equilibration dynamics. Instead of the pseudokinetic rearrangements including random bond breaking and re-formation, we used simple Wall–Mandel reptation,[13] which has the advantage of retaining monodisperse chain lengths and avoiding the polydispersity of pseudokinetic rearrangements. However, reptation equilibrates the system more slowly, especially at high concentration, and it is necessary to ensure that the system reaches true equilibrium. Each state in our simulation was equilibrated by as many as 3×10^8 reptation trial moves. The multichain configurations were analyzed and sampled into thermodynamic averages for each 5000 reptational moves.

The chain conformational properties in the bulk and at the interfaces were also investigated, including the components of the chain end-to-end distance perpendicular and parallel to the wall, i.e., $\langle R^2\rangle_\perp$ and $\langle R^2\rangle_\parallel$. These parameters reflect coil dimensions in the z direction, and in the x, y directions, respectively. In the bulk region, far from the wall or the surface, the ratio $\langle R^2\rangle_\parallel/\langle R^2\rangle_\perp$ should equal 2. In the simulation, a multichain configuration represented one sample of properties at a given distance z from the wall. Because the samples were averaged and the population of chains in principle also varied with z, our averages reflected not only conformational properties but also the chain population at z. Thus, the dimensions and the concentrations of the centers of the chains as a function of z obtained below are relative and not absolute quantities. However the $\langle R^2\rangle_\parallel/\langle R^2\rangle_\perp$ ratio, which was useful in the discussion, has an absolute quantitative meaning at any z. We also performed a simulation for one case in which the averaging at each z was performed separately; from this study we obtained absolute values for $\langle R^2\rangle_\parallel$ and $\langle R^2\rangle_\perp$. All coil dimensions and distances discussed in this work are in units of a cubic lattice of lattice spacing a.

We also investigated how the present results for a compressible system related to those obtained previously

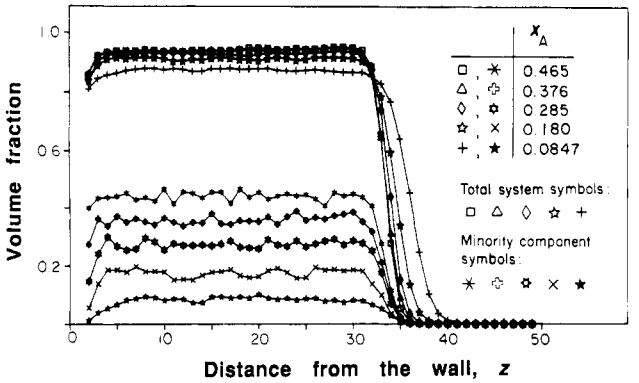

Figure 1. Volume fraction profile in the mixture as a function of distance from the wall (located at $z = 1$) for fixed interaction energy parameters $e_{AA} = e_{BB} = e_W = -0.5$ and $e_{AB} = -1.0$ and for variable composition.

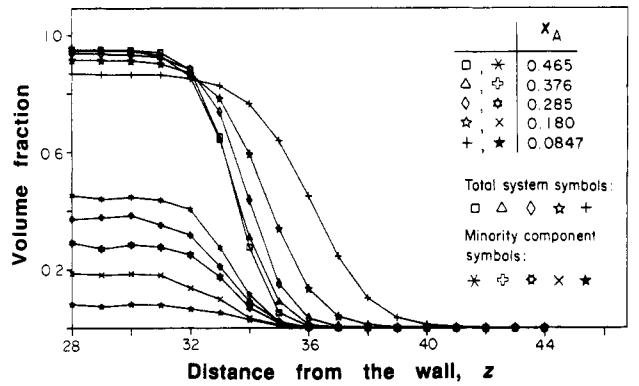

Figure 2. Volume fraction profile in the enriched surface layer. This figure represents an expansion of a portion of Figure 1, so the data and the parameters are identical to those given for Figure 1.

for fixed-concentration studies.[12] It is recognized, however, that there are certain differences in the two systems. In the open system, there were, for example, more representative interaction energies. In the fixed-concentration studies, separate assignment of cohesive energies e_{AA} and e_{BB} was unnecessary, because the chosen polymer concentration was constant. The reduced interaction energies e_{AB} in the two cases are not immediately comparable: in the open system, e_{AB} was shifted to more negative values because of the necessity of counteracting the cohesive energies to represent a given interaction parameter χ_{AB}. Most important, of course, the fixed-concentration studies did not take into account the compressibility of the system, particularly the dependence of the concentration of the condensed polymer phase on interaction energy.

III. Results and Discussion

A. Concentration and Blend Composition Profiles at the Interfaces. Figures 1–3 depict typical concentration profiles for the mixtures. The total concentration (of chains A and B) and the concentration of the minority component A, expressed as fractions of occupied volume, are shown as a function of the distance z from the wall located at $z = 1$. A broad region of constant-volume fraction lying between the surface of the blend and the wall interface is clearly visible in Figure 1. The value of the bulk concentration varies with the parameters e_{AB}, e_{AA}, and e_{BB} and the composition of the blend, because of the finite compressibility of the system. Such changes in bulk concentration are expected but also raise the question as to how closely the system corresponds to the compressibilities of real systems. The reduced nearest-neighbor interaction energy, a molecular parameter, is the basic

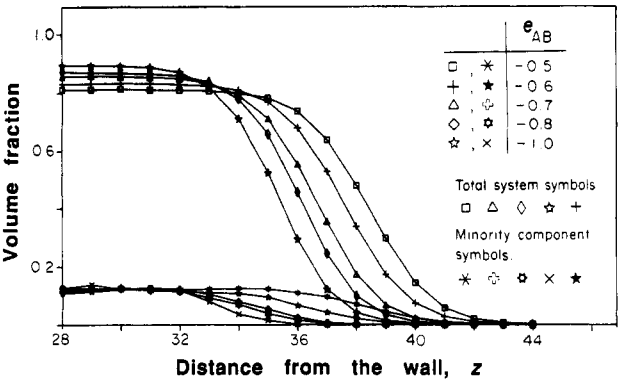

Figure 3. Surface enrichment at a fixed asymmetric composition $x_A = 0.130$ for several values of e_{AB}. The cohesive energies were fixed at $e_{AA} = e_{BB} = e_W = -0.5$.

variable and is responsible for substantial changes in overall system properties. When we apply equation-of-state theory, it can be shown that the present system in fact lies within the accessible experimental regime of typical polymers in this respect. [Using the usual terminology of equation-of-state theory, we define the reduced interaction energy as $e = T^*/T$, where $T^* \sim 6 \times 10^2$ K is one of the three close-packing nearest-neighbor molecular parameters. Calculating a volume expansion coefficient $\alpha = (\partial \ln (1/\phi(\infty))/\partial T)_P$ from our data for total bulk volume fraction $\phi(\infty)$, we obtain $\alpha \sim 0.5 \times 10^{-3}$ K^{-1}, a typical value for linear polymers.] The finite compressibility effects will be addressed in detail elsewhere.

The series of curves in Figures 1–3 also show the combined action of composition asymmetry and a favorable interaction energy e_{AB}, which (as will be shown below) must both be present to produce surface segregation. Figures 1 and 2 show how, for a fixed interaction corresponding to $\Delta e_{AB} = -0.5$, an enrichment of the surface layer with the majority component gradually develops as the overall composition becomes more asymmetric. It is observed that the inflection points of the total concentration profile and that of the corresponding minority component at the surface region move apart as the composition asymmetry of the system increases. Figure 3 depicts a similar situation in which the asymmetric composition is fixed at $x_A = 0.130$ and Δe_{AB} is varied from 0 to −0.5. Both series of curves in Figures 2 and 3 suggest that neither composition asymmetry at $\Delta e_{AB} = 0$ nor a highly favorable interaction in the absence of composition asymmetry can alone lead to segregation.

It should be noted that we generally used relatively highly favorable interactions (e.g., $\Delta e_{AB} = -0.5$, corresponding to a segmental interaction parameter $\chi_{AB} = -2$) because of the relatively short chains used in this calculation. For longer chains, lower χ_{AB} values would be appropriate to simulate the same region of miscibility/immiscibility characterized by the product $\chi_{AB}N$, where N is the chain length.

The surface of the respective polymer mixtures is characterized by diffuse concentration interfaces with the vacuum (solvent) (Figures 1–3). This profile $\phi(z)$ satisfies the familiar hyperbolic tangential equation[1,14,15]

$$\phi(z) = \frac{\phi(\infty)}{2}\left[1 - \tanh\left(\frac{z-d}{D}\right)\right] \qquad (1)$$

derived originally for polymer–polymer interfaces of incompatible polymer mixtures. In this expression $\phi(\infty)$ is the bulk volume fraction (total or value for either A or B component as appropriate), d is the location of the respective interface along the z axis, and D is the interfacial

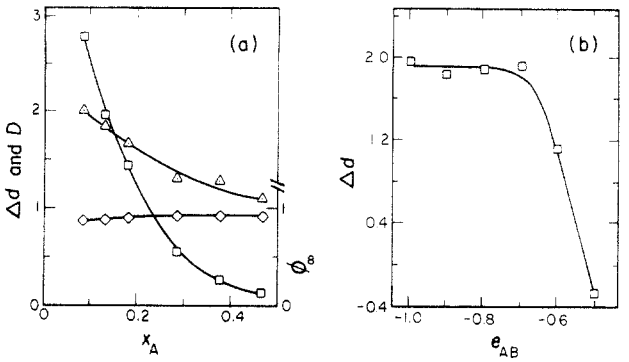

Figure 4. Surface segregation Δd calculated from eqs 1 and 2: (□) Δd; (△) D; (◇) $\phi(\infty)$. (a) Based on data shown in Figures 1 and 2: $e_{AA} = e_{BB} = -0.5$; $e_{AB} = -1.0$. (b) Based on data shown in Figure 3: $e_{AA} = e_{BB} = -0.5$; $x_A = 0.130$.

thickness. When fitting the surface profile to eq 1, we disregarded the low z (<10) region in calculating the surface parameters d and D and the bulk concentration $\phi(\infty)$. Results for both the total volume fraction and the minority component volume fraction were fitted to obtain the respective surface parameters for each state in Figures 1–3. The resulting parameters are shown in Figure 4. Surface segregation can be expressed as

$$\Delta d = d_T - d_A \tag{2}$$

where Δd is the distance between the surface for the total blend system, d_T, and the surface of the minority component, d_A. Figure 4a shows how the segregation develops as the composition becomes more asymmetric at constant $\Delta e_{AB} = -0.5$. For nearly symmetric composition, Δd approaches zero; for more asymmetric compositions, Δd increases steeply. Figure 4a also shows the total volume fraction of the system $\phi_T(\infty)$, which is slightly lower for asymmetric compositions than for symmetric compositions, because the heterocohesive energy e_{AB} exceeds the homocohesive energies $e_{AA} \equiv e_{BB}$. Similarly, the interfacial thickness D is larger for asymmetric compositions, with their more diffusive surfaces, than for symmetric ones.

Data for an asymmetric composition ($x_A = 0.130$) in which Δe_{AB} is varied from 0 to −0.5 is shown in Figure 4b. In the first case (Figure 4a), Δd increases rapidly as composition asymmetry increases; Figure 4b shows that, for the given large composition asymmetry, a relatively small change of Δe_{AB} is enough to introduce pronounced segregation (Δd). This effect, however, levels off as the interactions become increasingly favorable.

It is instructive to compare these observations with phenomenological mean-field theory.[1] Of course, with the present model, which is a system with no interaction between either of the components and the surface and with equal cohesive energies for both components ($e_{AA} = e_{BB}$), we cannot anticipate good agreement with MF theory, which is built on the assumption of different surface interactions for the components. It is convenient in this discussion to define a new coordinate system in which $z' = 0$ represents the location of the surface of the blend and $z' \gg 0$ denotes a point within the bulk composition. The composition profile of the blend under the surface ($z' > 0$) is defined in MF theory as

$$\frac{6z'}{a} = \int_{\phi(0)}^{\phi(z')} \left(\frac{d\phi}{\{\phi(1-\phi)[G(\phi,\chi) - G(\phi(\infty),\chi) - \Delta\mu(\phi - \phi(\infty))]\}^{1/2}} \right) \tag{3}$$

where $\phi(0)$ is the surface composition, G is the Flory–Huggins mixing free energy per site, $\phi(\infty)$ is the bulk composition (i.e., at $z' \gg 0$), and $\Delta\mu$ is the exchange potential related to G. The thickness of the enriched surface is expressed by

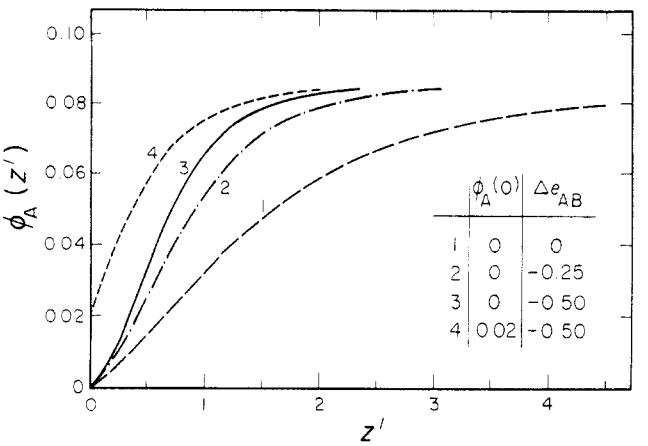

Figure 5. Composition profiles for minority components according to the phenomenological MF theory (eq 3) for the parameters $N = 30$ and $\phi(\infty) = 0.0847$ and for the surface composition $\phi(0) = 0$ with the interaction energies $\Delta e_{AB} = 0$, −0.25, or −0.5 and for the surface composition $\phi(0) = 0.02$ with interaction energy $\Delta e_{AB} = -0.5$.

$$z^* = \int_0^\infty (\phi(z') - \phi(\infty))\, dz' \tag{4}$$

The quantity z^* is thus similar to Δd defined in eq 2.

Equation 3 demonstrates an important difference between the MF approach and the present simulations. The MF treatment assumes that the total concentration of chains in the surface layers of the blend is constant and that only their composition varies. The present simulation shows that there is a diffuse concentration profile at the surface and that surface segregation occurs across the entire thickness represented by the smooth concentration profile. In other words, variation in both total concentration and composition must be considered simultaneously in the surface region of the blend.

All the blends exhibiting surface segregation considered here were highly miscible in the bulk state, with $\Delta e_{AB} < 0$. Such favorable energetics prevents phase separation, and a good intermixing of components is also implied. Phenomenological theory, on the other hand, predicts an increasing tendency toward surface segregation when the overall system approaches bulk phase separation, that is, in the vicinity of the binodal region. Clearly, the present observations and the predictions of MF theory exhibit opposite trends with respect to A–B interaction. This difference is well manifested in Figure 5, which depicts the application of eq 3 with parameters $N = 30$, $\Delta e_{AB} = 0$, −0.25, or −0.5, and $\phi(\infty) = 0.0847$ and for the surface compositions $\phi_A(0) = 0.0$ and 0.02. As noted before, the parameters $\phi_A(\infty)$ and $\phi_A(0)$ refer here to the concentrations of the minority component. The largest surface enrichment occurs with $\Delta e_{AB} = 0$, and it is less extensive for the more favorable interactions. Under these circumstances, there is no reason to speculate regarding the numerical difference between the maximum $\Delta d = 2.78$ obtained from MC simulation (Figure 4a) and the thickness of the enriched surface layer (~1.0) for the corresponding system in Figure 5.

The third difference between the present MC-based results and MF theory is that the latter predicts[1,6] that the maximum effect in surface segregation is for symmetric compositions, whereas we observe maximum effects for asymmetric compositions. These three important differ-

ences in MF predictions and MC results in these systems have led us to consider other possible mechanisms of surface enrichment beyond that predicted by the phenomenological MF theory.

The mean-field treatment[1] of a blend system suffers from the fact that it does not link the surface properties with bulk properties. In fact, it separates them and applies them to different regions. Mean-field theory predicts that the concentration profile below the surface is exclusively determined by the bulk properties of the mixture. The surface free energy differences only apply to the surface composition (i.e., at $z' = 0$) and truncate the general interfacial profile at this composition. Thus, the surface effects determine only which part of the general profile will actually form the surface region, whereas the shape of the concentration profile is fully determined by bulk properties. This property is documented by the central equation (eq 3) for this theory. As noted above, the surface composition $\phi(0)$ determined by surface free energy differences represents only a boundary condition.

As explained in the preceding paragraph, this treatment is appropriate for situations in which the surface free energy difference between components originates from interactions with the surface (and with other species above the condensed phase). Thus this treatment may not be a good approximation when the surface free energy differences arise only from the differences in bulk interactions e_{AA}, e_{BB}, and e_{AB} and from the composition of the blend, namely, when there is a strong link between the surface and bulk properties. The behavior represented by the results discussed here is for a system that has no surface interactions and in which surface demixing is driven solely by effects due to bulk interactions and the composition.

A simple argument using a lattice approximation can be given to rationalize the surface demixing in the present system. Consider a nearest-neighbor interaction that acts on the two components in the first layer ($z' = 0$) at the surface and is oriented toward the bulk region. If we assume a random mixing of components in the second layer ($z' = 1$), i.e., $\phi(\infty) = \phi(1)$, then component i in the first layer is subjected to a net nearest-neighbor interaction energy from the second layer, i.e.

$$e_i = \phi_i(\infty)e_{ii} + (1 - \phi_i(\infty))e_{ij} \quad \text{for} \quad i, j = \text{A, B}; i \neq j \tag{5}$$

where $\phi_i(\infty)$ is the volume fraction of component i in the bulk. With the values used earlier, $e_{AA} = e_{BB} = -0.5$ and $e_{AB} = -1.0$, we find that at symmetric composition both e_A and e_B are -0.75. However, for the asymmetric bulk composition $\phi_A(\infty) = 0.1$, this interaction is stronger for the minority component A ($e_A = -0.95$) than for the majority component B ($e_B = -0.55$). Of course, the random mixing picture for the second layer is only a first approximation; nevertheless this approximation indicates that there should be fewer minority chains in the surface region under these conditions. This is also seen in the MC simulation. It is also reasonable that the enriched surface layer for polymers is thicker than for a low-molecular-weight mixture and consists of more than one or two monomer layers.

B. Variation of Coil Dimension in Miscible Blends as a Source of Surface Segregation. The important effect that polymer coil size differences may have at the interface should be emphasized. Published results on the effect of blend interactions on the coil size of blend components at asymmetric compositions consider[16] the relative collapse of minority chains when unfavorable interactions are involved. There are also indications[17] of the opposite effect. If favorable interactions are present between components, then the minority chain coils expand if the other component has a "good solvent" quality. In the context of the present discussion the resulting difference in the size of the coils then gives rise to different behaviors for the two components in the surface layer: the larger coils are expelled from the surface to the bulk region and the smaller coils remain in an enhanced concentration in the surface layer.

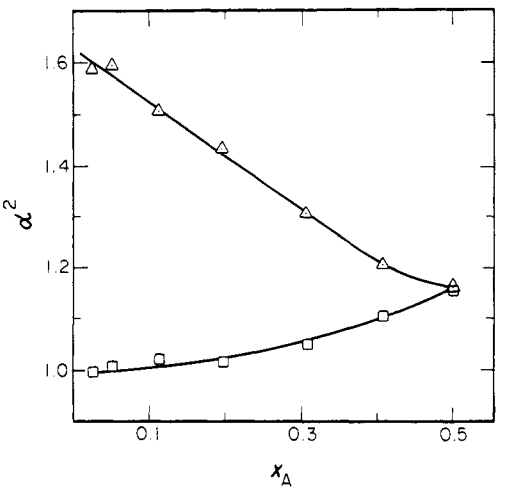

Figure 6. Variation of the coil expansion coefficient α^2 for minority (△) and majority chains (□) with composition x_A, for fixed $e_{AB} = -0.5$, calculated for an incompressible system with a total volume fraction of segments of 0.909. Reprinted, with permission, from ref 17.

Although the chain lengths of the A and B components in the present system are equal, the actual coil sizes are of course not necessarily equivalent. Figure 6 shows how coil size (in terms of coil expansion coefficient α^2) varies with composition. For a symmetric A/B blend composition, the thermodynamic conditions for both chain types are the same and coil sizes are necessarily equal. For asymmetric compositions, the minority chains expand while the coil size of the majority chains approaches the ideal unperturbed dimension. The parallel trends of a greater tendency to segregate and a greater difference in the coil size of the two components in asymmetric compositions indirectly support the idea that this segregation is driven by differences in coil sizes. In contrast, MF theory predicts a greater tendency toward segregation for symmetric compositions, as seen above. We note that the calculations for the data shown in Figure 6 were in fact performed, not by the method described in this paper, but by a canonical ensemble treatment used previously[12] to study bulk mixtures of somewhat shorter chains, $N = 20$, at constant total volume fraction of 0.909. This difference, however, does not in principle alter the observed effect. Note also that this coil expansion is not a marginal effect but is significant and readily measurable.

Figures 7 and 8 represent calculations of coil dimensions in a system for which $\Delta e_{AB} = -0.5$ and $x_A = 0.0847$, in terms of $\langle R^2 \rangle_\perp$ and $\langle R^2 \rangle_\parallel$ for both the majority and the minority components. Whereas in Figure 7 contributions to coil dimensions have been averaged and the data shown are relative, Figure 8 depicts absolute coil dimensions as mentioned above. A comparison of the bulk regions in the two figures reveals a considerable expansion of the minority relative to the majority coils. The expansion shown in Figure 8 is close to that of $\alpha^2 = 1.5$ seen in Figure 6 at $x_A = 0.1$. Also, it should be noted that coil dimensions in the bulk region agree closely with the ideal unperturbed

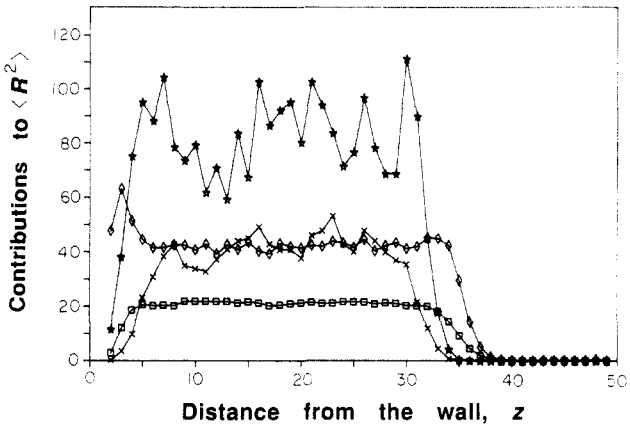

Figure 7. Contributions to the coil dimensions $\langle R^2 \rangle_\parallel$ and $\langle R^2 \rangle_\perp$ (see text). Symbols: for the majority components, $\langle R^2 \rangle_\perp$ (□), $\langle R^2 \rangle_\parallel$ (◇); for the minority components, $\langle R^2 \rangle_\perp$ (×), $\langle R^2 \rangle_\parallel$ (☆). Parameters: $e_{AA} = e_{BB} = e_W = -0.5$; $e_{AB} = -1.0$; $x_A = 0.0847$.

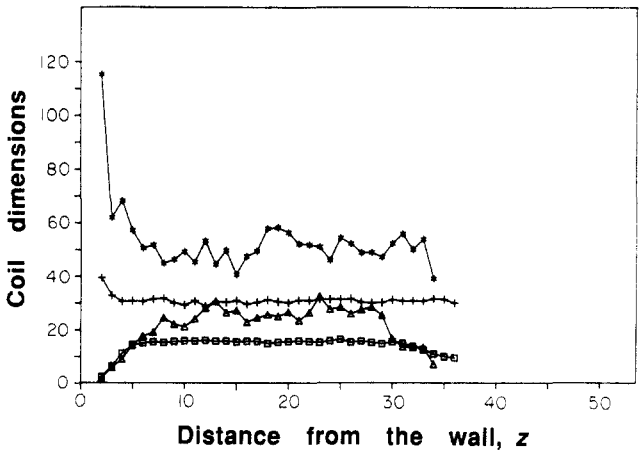

Figure 8. Absolute coil dimensions $\langle R^2 \rangle_\perp$ and $\langle R^2 \rangle_\parallel$ in a system with the parameters specified in Figure 7. Symbols: for the majority components, $\langle R^2 \rangle_\perp$ (□), $\langle R^2 \rangle_\parallel$ (+); for the minority components, $\langle R^2 \rangle_\perp$ (△), $\langle R^2 \rangle_\parallel$ (*).

ratio $\langle R^2 \rangle_\parallel / \langle R^2 \rangle_\perp = 2$, a further result indicating that these systems do not experience finite size effects.

The differences in coil sizes for the two components lead to different behavior at an interface: smaller coils preferentially occupy the interface. This behavior may be anticipated for two reasons. First, smaller coils (like small molecules) naturally tend to move to interfaces to increase miscibility and to raise the entropy at the interface. In studies of polymer–polymer interfaces for two polydisperse polymers, Olaj et al.[11] similarly observed that shorter chains move preferentially to the interface. In athermal polydisperse melts, shorter chains also preferentially occupy the surface, as recently predicted by Kumar et al.[6] Second, all coils are necessarily deformed at the surface, where they are geometrically constrained. Smaller coils can be located closer to the surface without deformation. The system can thus lower its overall free energy by increasing the concentration of the smaller coils at the surface layer. Kumar et al.[6] predicted that the excess of shorter chains at the surface should be on the order of 1% for strictly macromolecular systems in which only these entropic effects are involved. In the present system, we observed much larger effects because the enrichment is mainly energetically driven (in terms of Δe_{AB}), in agreement with Kumar et al.,[7] and also because the system involves relatively short macromolecular chains.

It is interesting to compare the thickness of the enriched layer with the dimensions of coils in the system. The maximal Δd obtained in Figure 4a is 2.78. The radii of gyration R_G of the minority and majority coils in the bulk region are respectively 3.5 and 2.8 for the same system, where these values are calculated from the usual expression $R_G = (\langle R^2 \rangle / 6)^{1/2}$. Thus, the initial assumption that the thickness of the enriched layer should be of the same order of magnitude as the size of the polymer coils is supported. The correspondence between the dimension of the enrichment layer and coil sizes is also consistent with the suggestion[6] that the size of the enriched layer depends in a simple fashion on the radius of gyration of coils and blend composition in an athermal blend with different chain lengths. In real systems, the thickness of the enriched layer might be of the order of 100 Å, and such an effect clearly represents a microphase separation.

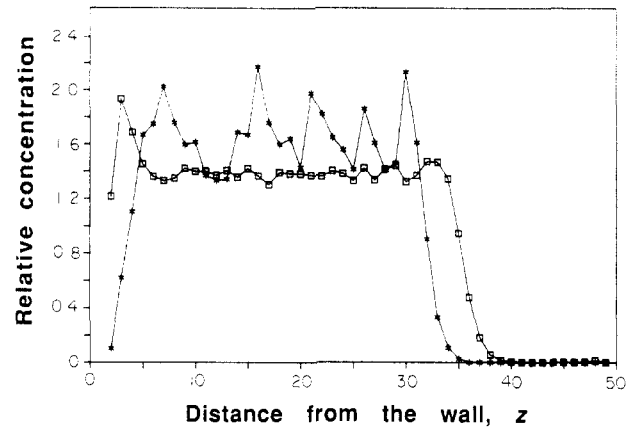

Figure 9. Relative concentrations of the centers of coil mass for majority (□) and minority (*) components. System parameters are the same as those specified in Figure 7.

C. Deformation and Orientation of Coils near the Interface. In this section, the above discussion regarding coil dimensions is extended to other regimes. For the bulk region, we reported undeformed coils with an $\langle R^2 \rangle_\parallel / \langle R^2 \rangle_\perp$ ratio corresponding to that of an unperturbed system, but this ratio is far from ideal at the two interfaces. For both the relative coil dimensions (Figure 7) and the absolute dimensions (Figure 8), the ratio is much larger than 2 in the interfacial regions. Coils near the interfaces are flattened in a direction parallel to the interface. This flattening is stronger at the wall than at the surface. Similarly, a smaller deformation at the surface than at the wall was reported for a polymer melt by Madden.[8] With the present results it is difficult to decide whether the deformation of the majority or the minority chains is greater. Generally, it can be observed that coils at the interface layer assume a flat, pancake conformation parallel to the surface.

Figure 9 depicts the relative concentration of the centers of coil mass for the majority and the minority components for systems with the same parameters used in the data developed in Figures 7 and 8. Two features are worth noting. The first is a considerable enrichment of coil centers of the majority chains both at the surface and at the wall. The second is a layering of coil centers near the surface and near the wall. This layering is stronger at the wall than at the diffusive surface of the blend. The maximum in the concentration of majority chains at the wall is somewhat closer to the wall than the radius of gyration of these coils in the bulk ($R_G = 2.8$) because the coils at the interfaces are flattened parallel to the interface. For the majority chains at the wall (Figure 9), our findings are generally close to those of Yoon et al.[18] and ten Brinke et al.,[19] namely, that the concentration of coil centers in polymer melts at the wall reaches a maximum at a distance comparable to the unperturbed R_G and the concentration

reaches its bulk value at a distance comparable to $2R_G$ from the wall.

D. Experimental Implications. Experimental studies to date have been carried out for nearly ideal polymer mixtures. We are not aware of any results on surface segregation in mixtures with favorably interacting components. Recently, however, studies were reported in which surface energy effects were combined with the effects of different chain lengths to enhance segregation.[3] As more information on chain behavior at the surface becomes available, the effects of this behavior will be better understood, and similarly, new surface experiments may prompt a detailed study of coils at interfaces. One report of interest is the recently observed[20] surface segregation in mixtures of linear and ring polymers having the same radius of gyration. In this system the surface is enriched preferentially by the linear chains—an observation that can be explained by the assumption of more degrees of freedom for the chain ends of linear chains. It is predicted from the work of Olaj et al.[11] that chain ends move preferentially to the interface at polymer–polymer interfaces; Yoon et al.[18] observed the same effect in athermal melts at the wall.

IV. Conclusions

Surface enrichment in polymer blends has been shown to be possible in a system in which there is no difference between surface interactions of components or cohesive energies of components and in which the components have equal chain lengths. The segregation occurs as a result of the blend composition and the interaction between the two components.

The concentration profile near the enriched surface is more complex than that predicted by MF theory. The blend surface has a diffuse concentration profile, and surface demixing occurs in parallel with this gradually changing concentration. Our results demonstrate the importance of also accounting for concentration variations at the surface, apart from composition variations.

Surface enrichment can be generally expected in the region of low mutual solubility in a mixture, close to the binodal region. Here we show an opposite trend. Deep in the one-phase region, a favorable interaction between the components in an asymmetric blend composition results in extensive changes in coil dimensions, and this is reflected in a surface enrichment. Of course, neither trend excludes the other, and both can be present and may superimpose in certain cases.

We wish to draw attention to this effect and to stimulate experiments on surface concentration profiles in miscible blends with favorable interactions as well as the development of an adequate theoretical background. The surface properties of complex materials are known to play a key role in a multitude of properties. Indeed, it is surprising that the surface of a blend that is miscible in the bulk can be formed almost exclusively by one of the components in certain cases. This result is especially intriguing in a blend where there are favorable interactions between the components but no preferential interactions of the components with the surface.

Acknowledgment. This work was supported by AFOSR Grant 92-001.

References and Notes

(1) Schmidt, I.; Binder, K. *J. Phys.* **1985**, *46*, 1631.
(2) Nakanishi, H.; Pincus, P. *J. Chem. Phys.* **1983**, *79*, 997.
(3) Composto, R. J.; Stein, R. S.; Felcher, G. P.; Mansour, A.; Karim, A. *Mater. Res. Soc. Symp. Proc.* **1990**, *166*, 485.
(4) Jones, R. A. L.; Kramer, E. J.; Rafailovich, M. H.; Sokolov, J.; Schwarz, S. A. *Phys. Rev. Lett.* **1989**, *62*, 280.
(5) Composto, R. J.; Stein, R. S.; Jones, R. A. L.; Kramer, E. J.; Felcher, G. P.; Karim, A.; Mansour, A. *Phys. B* **1989**, *156 & 157*, 434.
(6) Hariharan, A.; Kumar, S. K.; Russell, T. P. *Macromolecules* **1990**, *23*, 3584.
(7) Hariharan, A.; Kumar, S. K.; Russell, T. P. *Macromolecules* **1991**, *24*, 4909.
(8) Madden, W. G. *J. Chem. Phys.* **1987**, *87*, 1405.
(9) Sariban, A.; Binder, K. *J. Chem. Phys.* **1987**, *86*, 5869.
(10) Sariban, A.; Binder, K.; Heermann, D. W. *Colloid Polym. Sci.* **1987**, *265*, 424.
(11) Reiter, J.; Zifferer, G.; Olaj, O. F. *Macromolecules* **1990**, *23*, 224.
(12) Cifra, P.; Karasz, F. E.; MacKnight, W. J. *J. Polym. Sci., Polym. Phys.* **1988**, *26*, 2379.
(13) Wall, F. T.; Mandel, J. *J. Chem. Phys.* **1975**, *63*, 4592.
(14) Cahn, J. W.; Hilliard, J. E. *J. Chem. Phys.* **1958**, *28*, 258.
(15) Helfand, E.; Tagami, Y. *J. Chem. Phys.* **1972**, *56*, 3592.
(16) Sariban, A.; Binder, K. *Macromolecules* **1988**, *21*, 711.
(17) Cifra, P.; Karasz, F. E.; MacKnight, W. J. *Macromolecules* **1992**, *25*, 192.
(18) Kumar, S.; Vacatello, M.; Yoon, D. Y. *J. Chem. Phys.* **1988**, *89*, 5206.
(19) ten Brinke, G.; Hadziioannou, G.; Ausserre, D.; Hirz, S.; Frank, C. *Bull. Am. Phys. Soc.* **1988**, *33*, 498.
(20) Composto, R. J. Private communication.